Analysis and Development of an Improved Y-source Boost DC-DC Converter

Mojtaba Forouzesh, Alfred Baghramian

Department of Electrical Engineering, University of Guilan, Rasht, IRAN
m.forouzesh.ir@ieee.org, alfred@guilan.ac.ir

Abstract: Y-source impedance network is a new topology intended for implementing with high voltage gain converters. In contrary to the original Y-source impedance network, an improved Y-source presented in this paper has the advantage of a continuous input current characteristic. Since achieving high voltage gain and continuous input current, converters employing the proposed impedance network are suitable for implementing with renewable energy sources like fuel cell and photovoltaic systems. In this paper, analysis and operation principles of the developed network have been discussed. Moreover, mathematical equations and input current ripple analysis have been demonstrated in detail. Finally, both computer simulations and experimental results from a boost dc-dc converter are presented to validate the performance of the developed network.

Keywords: DC-DC power converter, high voltage boost, Y-source, magnetically coupled impedance source (MCIS), continuous input current.

1. Introduction

Recently, due to shortage of fossil fuels, alternative energy like renewable sources are in the center of attention. Among them fuel cell (FC) and photovoltaic (PV) systems because of no sound and emission characteristics are more desirable. Output voltage of these sources are environmentally dependent and can vary in a wide range. Thus, in order to cover dc-link voltage requirements, the need for a power electronics converter is undeniable. As mentioned above, in some conditions output voltage of both FC and PV can be such low that a converter with high voltage gain should be used [1]. Up to now, researchers have investigated various dc-dc converters with different structures. In order to meet dc link voltage requirements, there is demand for a high voltage gain converter when operating with low voltage sources. In a conventional dc-dc boost converter due to efficiency and reliability problems, a high voltage gain is not achievable. In transformer based converters usually a large turn ratio must be utilized to achieve a high voltage gain. Large turn ratios may lead to high leakage inductances and hence large voltage spike on semiconductor devices. Multilevel and interleaved converters usually use large amount of components that increase size and cost of converters. In addition, multilevel converters may not be desired for power conditioning systems due to their complex control algorithms and large components count [2, 3].

Recently coupled inductors are widely used in power converters. By utilizing coupled inductors, dc-dc converters usually can achieve high voltage gain with lower components [4-8]. Another application of coupled inductors is in magnetically coupled impedance networks. These networks called impedance sources that their generation initiated with the Z-source inverter in 2003 [9]. In recent years, many impedance sources have been developed for implementing on either dc/ac inverters or dc-dc converters. Originally, voltage gain of the Z-source and quasi-Z-source networks are low to be implemented with renewable energy power conditioning systems. Hence, improving Z-source based converter characteristics have been investigated [10-13]. Magnetically coupled impedance networks that appear recently, can achieve high voltage gain with lower components count. Some of dominant networks in this category can be named as trans-Z-source [14], Γ-source [15] and Y-source [16].

Received: May 25th, 2015. Accepted: March 17th, 2016
DOI: 10.15676/ijeei.2016.8.1.14

Due to the presence of an input diode in mentioned impedance networks, these networks inherently suffer from discontinuous input current. Whereas, a continuous input current trait is an important feature for converters operating with renewable energy sources like FC and PV systems. In a fuel cell system, drawing discontinuous input current lead to higher hydrogen consumption, hence the efficiency of FC diminishes [17]. On the other hand, converters with continuous input current can operate more accurately around the maximum power point in a photovoltaic system [18]. Thus, it is noticeable that the efficiency of both FC and PV can be improved by utilizing converters with a continuous input current. Besides drawing chopping input current from FC and PV has negative influence on their lifetimes [17, 18]. Therefore, converters with continues input current are always attractive due to their reducing negative impact on the DC input source. Some investigations have been done in order to achieve a continuous input current on magnetically coupled impedance sources. In these papers, usually large filter inductor and capacitor were added to the original network [19, 20]. In fact, adding large passive elements to the circuit results in more cost and weight (size) of power converters that it is not desirable.

The Y-source impedance network can achieve high voltage gains in small duty cycles. In contrary to other mentioned magnetically coupled networks, the Y-source utilizes three coupled inductors that gives it more design freedoms. In this paper, an improved Y-source network with a continuous input current is proposed for dc-dc converters. The proposed impedance network not only has all the merits of original Y-source network but also has a continuous input current. Moreover, the novel method introduced for achieving a continuous input current on the Y-source can easily be extended to other magnetically coupled impedance sources. In the proposed method, only one small value capacitor is added to the circuit of the original network. Figure 1 shows some possible dc-dc converter architectures for the improved Y-source impedance network. As it can be seen, the improved Y-source network can be implemented on either a full bridge dc-dc structure or a single switch boost dc-dc converter. Indeed, an improved Y-source based isolated dc-dc converter is under investigation by the authors [21].

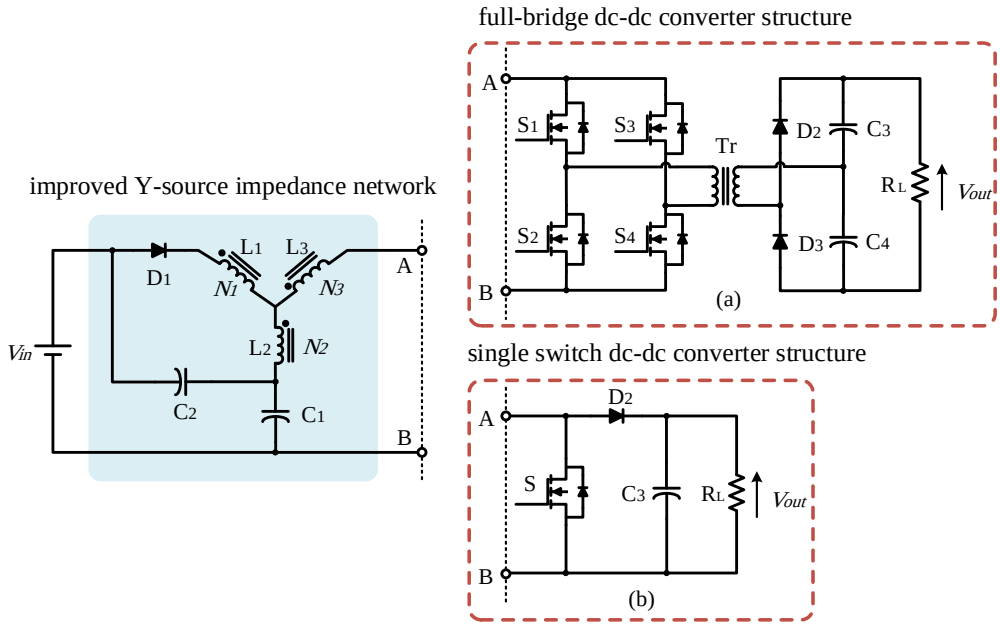

Figure 1. The proposed Y-source based dc-dc converter, (a) with full bridge isolated structure and (b) with single switch boost structure.

This paper is organized as follows. In section II, development of the improved Y-source impedance network is demonstrated. In first, a review of the Y-source network and its counterpart quasi-Y-source network have been presented. Subsequently, analysis and principals of the improved impedance network have been discussed. In addition, their corresponding equations have been derived in this section. In section III, the proposed high voltage gain network with a continuous input current is implemented on a boost dc-dc converter. Furthermore, input current ripple analysis and a comparison with other converters are demonstrated in this section. In section IV, the performance of discussed networks verified with the aid of PSIM simulations. The derived mathematical equations and expected waveforms are also validated by simulation results. In section V, experimental results from a laboratory prototype are illustrated to verify mentioned features of the proposed converter. Finally, the conclusion is presented in the last section.

2. Operation Principles and Mathematical Derivations

A. Y-source impedance network

The conventional Y-source impedance network and its equivalent circuits are depicted in Figure 2. It should be noted, since the effect of leakage inductance on the performance of magnetically coupled Y-source network have been studied with introducing an additional intermediate operating mode [22]. In this paper, in order to facilitate the analysis of in this section, a perfect coupling is considered for the coupled inductors of all impedance networks. Considering the latter mentioned, like other conventional impedance networks, the Y-source impedance network has two basic operating modes, the shoot-through and non-shoot-through modes. When switch S is turn ON the shoot-through sate starts in which diode D is in revers bias and capacitors C_2 is discharging to the magnetizing inductance of the coupled inductors. The equivalent circuit of this mode is shown in Figureb. With the assumption that the voltage across inductor L_1 is V_L, then the voltage across L_2 is V_L/n_{12} and voltage across L_3 is V_L/n_{13}, which $n_{12} = N_1/N_2$ and $n_{13} = N_1/N_3$ are the turn ratios of the three winding coupled inductors. By applying Kirchhoff's Voltage Law (KVL) in both modes and writing voltage-second balance principle for the inductor L_1, the voltage across capacitor C_2 and the voltage gain of the Y-source impedance network can be achieved as follows.

$$V_{C2} = \frac{1-d_{ST}}{1-\left(\frac{N_3+N_1}{N_3-N_2}\right)d_{ST}} V_{in} \tag{1}$$

$$\frac{V_{out}}{V_{in}} = \frac{1}{1-\left(\frac{N_3+N_1}{N_3-N_2}\right)d_{ST}} \tag{2}$$

In (4), d_{ST} is the shoot-through duty cycle. In order to simplify the equations, a winding factor can be defined as $K = \frac{N_3+N_1}{N_3-N_2}$. Therefore, (1) and (2) can be rewritten as

$$V_{C2} = \frac{1-d_{ST}}{1-Kd_{ST}} V_{in} \tag{3}$$

$$\frac{V_{out}}{V_{in}} = \frac{1}{1-Kd_{ST}} \tag{4}$$

In order to achieve positive boost characteristics for the Y-source impedance network, denominator of (4) should be between zero and one. Thus, the available shoot-through duty cycle can be obtained.

$$0 < 1 - Kd_{ST} < 1 \;\rightarrow\; 0 < d_{ST} < \frac{1}{K} \tag{6}$$

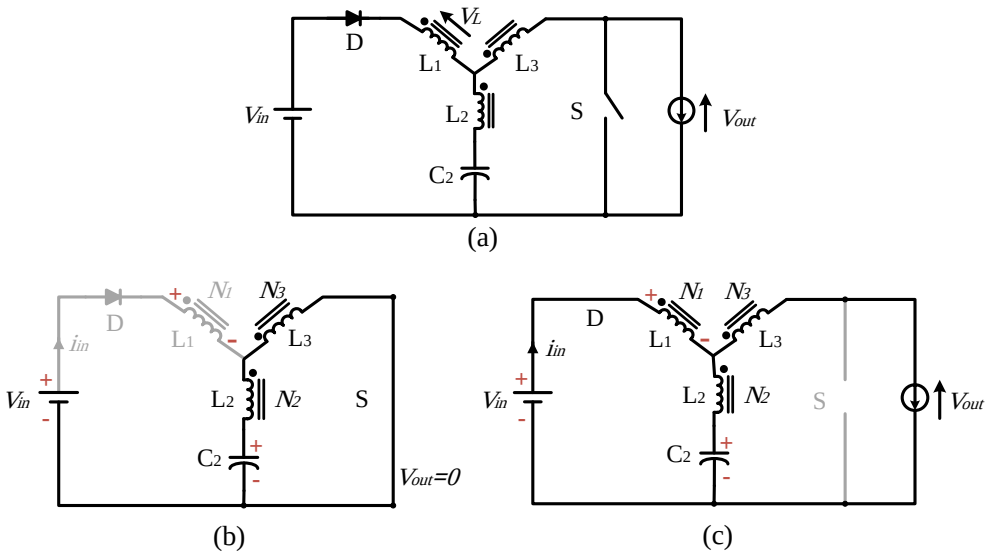

Figure 2. The Y-source impedance network and its equivalent circuit in (b) the shoot-through state and (c) the non-shoot-through state

B. Quasi-Y-source impedance network

$$V_{C1} = \frac{\left(\frac{N_1+N_2}{N_3-N_2}\right)d_{ST}}{1-\left(\frac{N_3+N_1}{N_3-N_2}\right)d_{ST}} V_{in} \tag{7}$$

By substituting the winding factor K in (7), it can be rewritten as

$$V_{C1} = \frac{(K-1)d_{ST}}{1-Kd_{ST}} V_{in} \tag{8}$$

$$\frac{V_{out}}{V_{in}} = \frac{1}{1-Kd_{ST}} \tag{9}$$

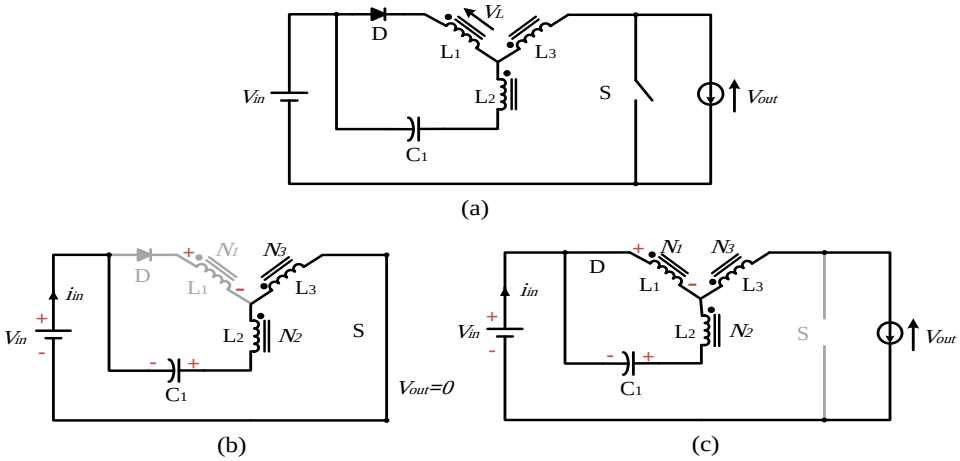

Figure 3. The quasi-Y-source impedance network and its equivalent circuit in (b) the shoot-through state and (c) the non-shoot-through state

Energy storage capacitor of the original Y-source impedance network can be replaced as shown in Figure 3. This new impedance network called as quasi-Y-source. The quasi-Y-source network operates mostly like the Y-source network but they have some differences in capacitor voltage stress and input current waveform. The equivalent circuit of the shoot-through mode is shown in Figure 3b. In this mode, the magnetizing inductance of the coupled inductors is charging form both input source and capacitor C_1. Writing KVL in both modes then applying voltage-second balance to the inductor L_1, the voltage across capacitor C_1 and the voltage gain of the quasi-Y-source impedance network can be obtained.

It is obvious that the voltage gain of two latter networks are equal but their capacitors voltage stress are different. Considering (3) and (8), the normalized voltage stress across storage capacitors of two mentioned impedance network for a specific winding factor are drawn in Figure 4. It is obvious that in every duty cycle and voltage gain, the voltage stress across storage capacitor of the quasi-Y-source is lower than the Y-source impedance network.

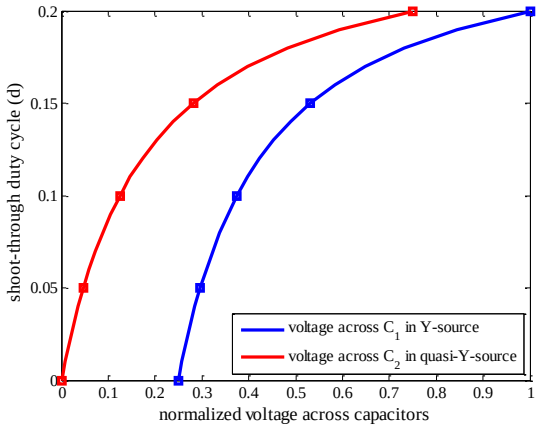

Figure 4. Comparison between normalized capacitors voltage stress.

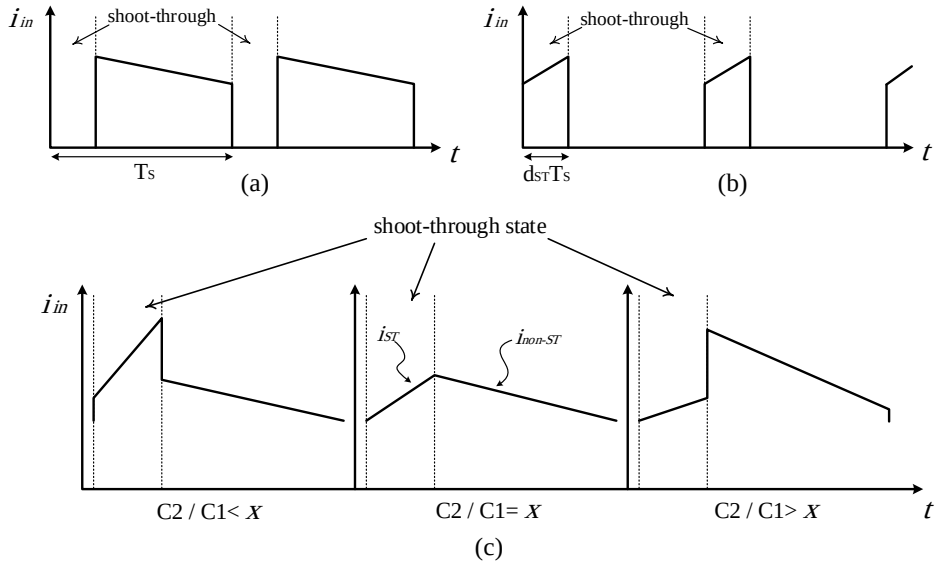

Figure 5. Expected input current waveforms for (a) Y-source impedance network, (b) quasi-Y-source impedance networks and (c) the improved Y-source impedance network with different capacitors ratios

Expected input current waveform for the Y-source, quasi-Y-source and the improved Y-source impedance networks are shown in Figure 5. The input current in both Y-source and quasi-Y-source networks is discontinuous. In fact, the input current ripple in quasi-Y-source network is more that in Y-source network. In the next section, a novel Y-source impedance network with a continuous input current is presented. Figure 5c illustrates the input current waveform of the proposed impedance network with different capacitor ratios (C_1 and C_2). To achieve a continuous input current with no current jump in transition between two operation modes, a proper capacitors ratio (x) should be considered for the improved Y-source impedance network.

C. improved Y-source impedance network

Figure 6 illustrates the improved Y-source impedance network and its equivalent circuits in both modes. The improved Y-source network combines the two storage capacitors of the Y-source and quasi-Y-source impedance networks. In the proposed Y-source network, a continuous input current can be achieved with special consideration of the value of capacitors C_1 and C_2. Proper selection of the capacitors will be shown in the following of this section. Like aforementioned networks, in the shoot-through mode diode D is in reverse bias, in this mode capacitors C_1 and C_2 are charging the magnetizing inductance of the coupled inductors. Applying KVL in this mode, the following equations can be obtained.

$$V_{C2} = V_{in} + V_{C1} \tag{11}$$

$$V_L = \frac{n_{12}n_{13}}{n_{12}-n_{13}} V_{C2} \tag{12}$$

The non-shoot-through mode starts while diode D is conducting and capacitors C_1 and C_2 are charging from the input source. By applying KVL in this mode, the following equations can be written.

$$V_L = \frac{n_{12}}{1+n_{12}} V_{C2} \tag{13}$$

$$V_{out} = V_{in} - V_L - \frac{V_L}{n_{13}} \tag{14}$$

Applying voltage-second balance principle to the inductor L_1 and considering (11)-(14), voltage across capacitors C_1, C_2 and the output voltage of improved Y-source network can be achieved as follows.

$$V_{C1} = \frac{(1-d_{ST})}{1-\left(\frac{N_3+N_1}{N_3-N_2}\right)d_{ST}} V_{in} \tag{15}$$

$$V_{C2} = \frac{\left(\frac{N_1+N_2}{N_3-N_2}\right)d_{ST}}{1-\left(\frac{N_3+N_1}{N_3-N_2}\right)d_{ST}} V_{in} \tag{16}$$

$$V_{out} = \frac{V_{in}}{1-\left(\frac{N_3+N_1}{N_3-N_2}\right)d_{ST}} \tag{17}$$

It is clear that the calculated equations for the voltage across C_1 and C_2 and output voltage of the improved Y-source is same as which calculated for both previous networks.

From derivative of (14), the relation between currents of capacitor C_1 and C_2 can be achieved.

$$dV_{C2} = dV_{C1} \rightarrow i_{C2} = \frac{C_2}{C_1} i_{C1} \tag{18}$$

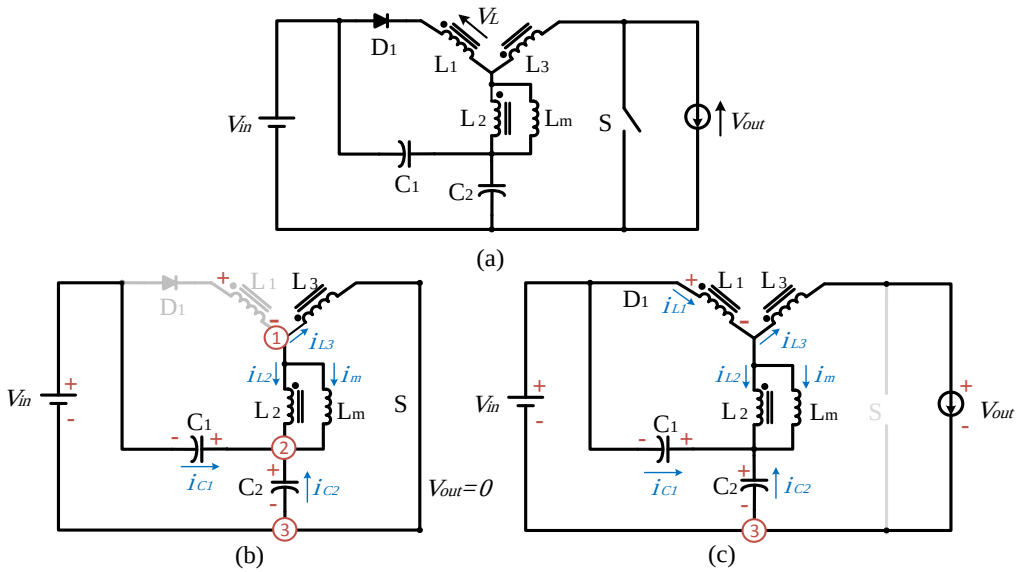

Figure 6. The improved Y-source impedance network and its equivalent circuit in (b) the shoot-through state and (c) the non-shoot-through state

Assuming that the network operates in its continuous conduction mode (CCM), the average of magnetizing current in both shoot-through and non-shoot-through modes equals to the average of magnetizing current in a switching period. According to Figure 5c, in order to achieve a continuous input current with no current jump in transition between two modes, the dc component of input current (I_{dc}) should be equal to the average of input current in either shoot-through or non-shoot-through mode.

$$I_{dc} = I_{in_{ST}} = I_{in_{non-ST}} \tag{19}$$

In (22), I_{in} denotes the average of input current and subscripts 'ST' and 'non-ST' represent the shoot-through and non-shoot-through modes, respectively. Assuming that the improved Y-source is loss less ($P_{in} = P_{out}$) and according to (17), the output current can be written as follows.

$$I_{out} = \left(1 - \left(\frac{N_3 + N_1}{N_3 - N_2}\right) d_{ST}\right) I_{dc} \tag{20}$$

Ampere-turns balance in a three winding coupled inductors can be expressed as

$$N_1 i_{L1} + N_2 i_{L2} + N_3 i_{L3} = 0 \tag{21}$$

In the shoot-through mode, i_{L1} current of L_1 is zero. Applying Kirchhoff's Current Law (KCL) at nodes 1, 2 and 3 in Figure 6b and considering (18) and (20), the following equations can be written.

$$i_{ST} = \left(\frac{N_2}{N_3 - N_2}\right) i_m \tag{22}$$

$$i_m = \left(\frac{N_3 - N_2}{N_2}\right)\left(\frac{C_2}{C_1} + 1\right) i_{in_{ST}} \tag{23}$$

$$i_{C2} = \left(\frac{N_2}{N_3 - N_2}\right) i_m - i_{in_{ST}} \tag{24}$$

In (22), i_{ST} is the shoot-through current that flows into the semiconductor switch and i_m is the magnetizing current referred to the second winding (N_2). In the non-shoot-through mode, considering (20) and by applying KCL at node 1 in Figure 6c, the following equation can be written.

$$i_{C2} = \left(1 - \left(\frac{N_3 + N_1}{N_3 - N_2}\right) d_{ST}\right) I_{dc} - i_{in_{non-ST}} \tag{25}$$

By considering small ripple for i_m, $i_{in_{ST}}$ and $i_{in_{non-ST}}$, they can be expressed by their average values I_m, $I_{in_{ST}}$ and $I_{in_{non-ST}}$, respectively. Applying ampere-second balance principle to the capacitor C_2, dc component of the magnetizing current for improved Y-source network can be obtained as

$$I_m = \left(\frac{N_1 + N_3}{N_2}\right) I_{dc} \tag{26}$$

By substituting (26) in (22), the average of shoot-through current in Y-source network can be achieved as

$$I_{ST} = \left(\frac{N_3 + N_1}{N_3 - N_2}\right) I_{dc} = K I_{dc} \tag{27}$$

Considering (19) and using (23) and (26), the proper capacitance ratio for the Y-source network can be achieved.

$$\frac{C_2}{C_1} = K - 1 \tag{28}$$

3. Implementation of the Proposed DC-DC Converter

By having the advantage of high voltage boost and continuous input current abilities, the improved Y-source impedance network is suitable for implementing with low input voltage dc-dc converters. The dc-dc boost converter proposed in this paper is a simple example to show the performance of the improved Y-source network. Input current analysis and comparison with other dc-dc converters are discussed in this section.

A. Principle of Operation

Figure 7 shows the configuration of the test system, where an improved Y-source impedance network has been replaced with the input inductor of a boost dc-dc converter. The shoot-through state can happens by turn ON of switch S, in which diode D_1 and D_2 are in reveres bias. In this mode, input source and capacitors C_1 and C_2 are charging the magnetizing inductance of the coupled inductors. Moreover, the resistive load is supplied by the capacitor C_3 in this mode. When the switch S is turned OFF, impedance network is in its non-shoot-through mode. In which the capacitors are charging from the input source and capacitor C_3 is

supplied by the stored energy in coupled inductors and input source. This happens only if the peak of output voltage ($\hat{V}_{out}$) is lower that the peak of ($\hat{V}_{ds}$).

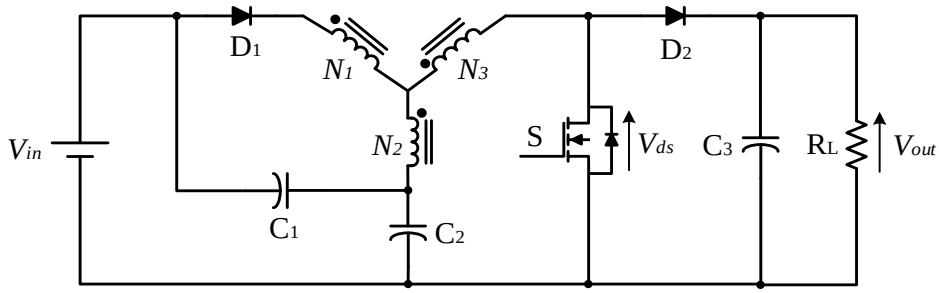

Figure 7. The improved Y-source boost dc-dc converter

According to (17), in the proposed converter different winding turn ratios ($N_1: N_2: N_3$) can be realized for a specific voltage gain. Considering (26), it is interesting that the required magnetizing current for a specific voltage gain in the proposed Y-source based converter can vary by various selection of winding turn ratios. This is another design freedom for the Y-source impedance network in addition to other advantages mentioned in [16]. Table 1 shows some different combinations of winding turns for specific winding factors and their corresponding magnetizing current and voltage gain.

Table 1. Different magnetizing current and voltage gain of the Y-source impedance network realized with different winding factor and turns ratio

Winding Factor ($K = \frac{N_3+N_1}{N_3-N_2}$)	Turns Ratio ($N_1: N_2: N_3$)	Magnetizing Current ($I_m = \frac{N_1+N_3}{N_2} \times I_{dc}$)	Voltage Gain ($\frac{V_o}{V_{in}} = \frac{1}{1-Kd_{ST}}$)
3	1:3:5	$2 \times I_{dc}$	$\frac{1}{1-3d_{ST}}$
	1:1:2	$3 \times I_{dc}$	
	3:1:3	$6 \times I_{dc}$	
4	1:2:3	$2 \times I_{dc}$	$\frac{1}{1-4d_{ST}}$
	2:1:2	$4 \times I_{dc}$	
	5:1:3	$8 \times I_{dc}$	
5	1:3:4	$2.5 \times I_{dc}$	$\frac{1}{1-5d_{ST}}$
	3:1:2	$5 \times I_{dc}$	
	7:1:3	$10 \times I_{dc}$	

B. Analysis of Input Current and Magnetizing Current Ripples

The Input current of the proposed network is a ratio of the magnetizing current of coupled inductors. Therefore, the input current ripple can be evaluated from the magnetizing current ripple. For the following analysis, inductors and capacitors are assumed to be linear and frequency independent. Accordingly, the voltage across magnetizing inductor on the second winding (N_2) can be achieved using KVL in the non-shoot-through mode.

$$V_{Lm} = \left(\frac{N_2}{N_1+N_2}\right) V_{C1} \tag{29}$$

Then, the magnetizing current for the improved Y-source can be expressed as (30)

$$i_{Lm} = \frac{1}{L_m} \int_{d_{ST}T}^{t} V_{Lm}\, dt + i_{Lm}(0) \tag{30}$$

$$\rightarrow = \frac{V_{Lm}}{L_m}(t - d_{ST}T) + i_{Lm}(0)$$

In (30), L_m is the magnetizing inductance seen from the second winding (N_2) of coupled inductors. Considering (29) and (30), the magnetizing current ripple of improved Y-source network can be written as

$$\Delta i_{Lm} = \left(\frac{{N_2}^2}{N_1N_2+{N_2}^2}\right) \cdot \frac{V_{C1}(1-d_{ST})}{L_m f_s} \tag{31}$$

According to (29), the input current ripple for the improved Y-source can be obtained as

$$\Delta i_{in} = \left(\frac{{N_2}^2}{(N_1+N_2)(N_1+N_3)}\right) \cdot \frac{V_{C1}(1-d_{ST})}{L_m f_s} \tag{32}$$

Considering Table 1 and equation (32), it is evident that with a specific voltage gain for the improved Y-source, the input current ripple can differ by various windings turns. This feature is only provided by the improved Y-source impedance network, which is not seen on other magnetically coupled impedance networks yet.

C. Comparison With Other DC-DC Converters

Several high voltage dc-dc converters have been investigated for various applications. Among them, few converters can achieve a continuous input current and high voltage boost simultaneously. A comparison of different dc-dc converters in terms of their components and voltage gains are presented in Table 2.

Table 2. Comparison of Various DC-DC Converters

Reference	Voltage Gain	Continuous Input Current	Number of Components				
			Switch	Diode	Inductor	Capacitor	Total
[4]	$\frac{(1+n)D}{1-D}$	no	1	2	2	2	7
[5]	$\frac{1}{(1-D)^2}$	yes	2	3	2	3	10
[6]	$\frac{1+nk}{1-D}$	no	1	3	2	3	9
[8]	$\frac{(2+nD)}{1-D}$	no	1	4	2	4	11
[13]	$\frac{1}{1-2D}$	yes	1	1	3	2	7
[10]	$\frac{2(1-D)}{1-3D}$	yes	1	3	4	4	12
Proposed Converter	$\frac{1}{1-KD}$	yes	1	2	3	2	8

From Table 2 it is obvious that the proposed converter can achieve high voltage gain with relatively low number of circuit components. For better illustration, a comparison between voltage gain of some mentioned dc-dc converters are drawn in Figure 8. It can be pointed out that the comparison is made between converters with continuous input current characteristics. It is obvious that the proposed Y-source based dc-dc converter can achieve higher voltage gains with lower duty cycles. This feature of the proposed configuration makes it adequate for applications that demand for short inductive charge.

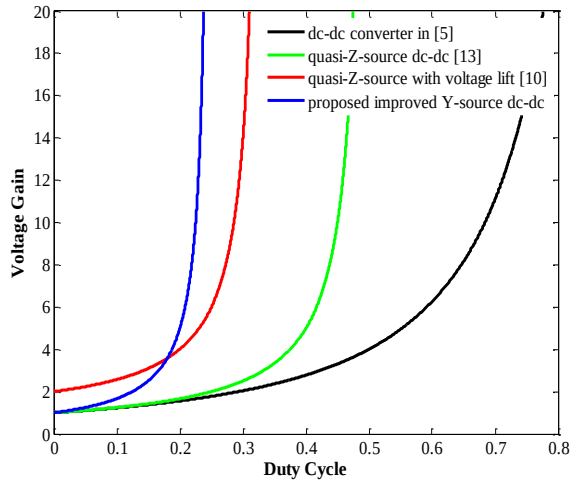

Figure 8. Comparison between voltage gain of the proposed converter and other converters

4. Simulation Results

For demonstrating the performance of mentioned impedance networks, some simulations have been done in the PSIM software environment. Three coupled inductors ratio assumed to be 2:1:2 ($N_1 : N_2 : N_3$). Thus, winding factor can be calculated as K=4. Considering a 40V input voltage and a 200V output voltage, the voltage gain of the proposed converter should be about 5. From (2), the required shoot-through duty cycle can be calculated as d_{ST}=0.2. Considering (28), proper ratio for the capacitors should be 3 and hence C_1 and C_2 was selected 100µF and 300µF respectively. From (15) and (16), the voltage across capacitors C_1 and C_2 were calculated as V_{C1}=120V and V_{C2}=160V respectively.

First, the simulations have done to verify the differences between the Y-source and quasi-Y-source networks that mentioned earlier. Consequently, they were implemented on boost dc-dc converters like the configuration shown in Figure 7. In this case, the same 300µF capacitor is used for both networks. Simulation results for both converters are drawn in Figure 9. It can be seen that the peak value of input current for quasi-Y-source is higher than its counterpart. Because of this behavior that seen form two mentioned networks, in the improved Y-source network, we have to consider a special ratio for two storage capacitors to achieve a continuous input current with less ripple.

Simulation results for the improved Y-source boost dc-dc converter are depicted in Figure 10. It can be seen that the input current is continuous in the proposed converter and its ripple can be tuned by both the switching frequency and the magnetizing inductance. The voltages stress across capacitors C_1 and C_2 that are shown in Figure 10 are in good agreement with the calculated values. From Table 1 and considering (32), it is found that for a specific voltage gain, the input current ripple of the proposed converter can be lowered by different winding turns ratios ($N_1 : N_2 : N_3$). In order to conduct a practical comparison for the currents analysis, it is assumed that the magnetizing inductance seen form the winding with the lowest turns is 200 µH for all windings combinations.

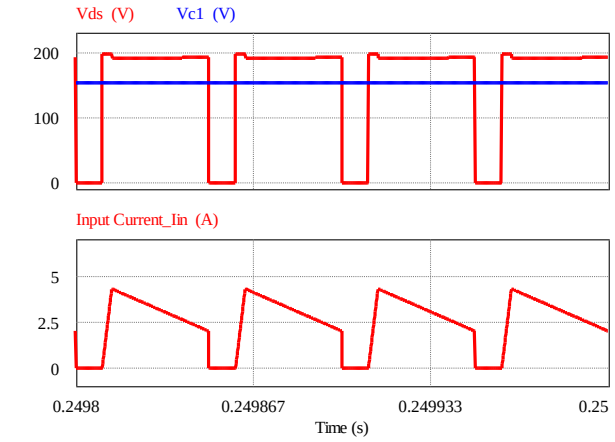

(a)

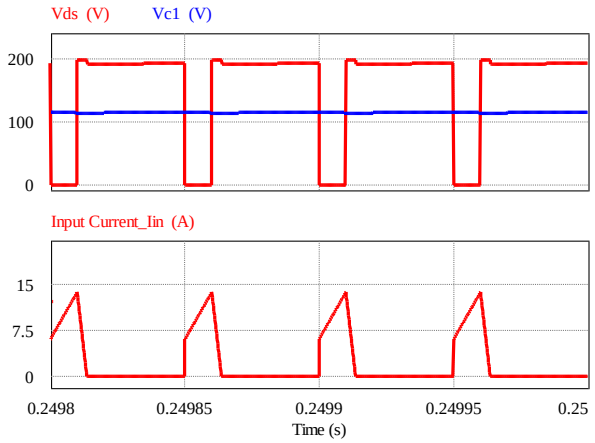

(b)

Figure 9. Steady state respond for (a) Y-source boost dc-dc converter and (b) quasi-Y-source boost dc-dc converter.

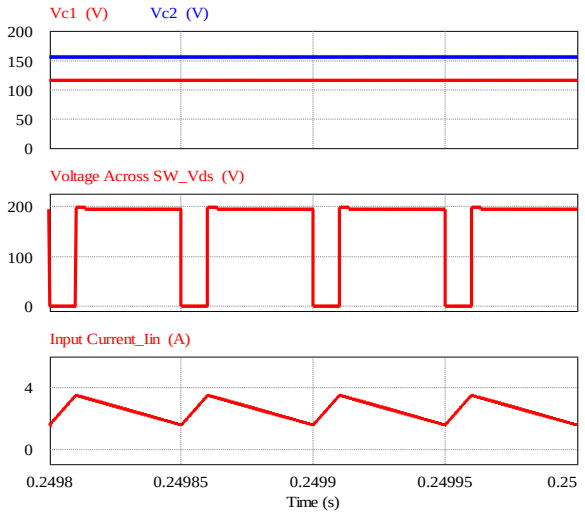

Figure 10. Simulation results for the improved Y-source boost dc-dc converter in steady state.

Figure 11 illustrates the simulation results for the input current and magnetizing current with different combinations of winding turns. In other to achieve K=4, three turns ratios are mentioned in Table 1. Current ripples drawn in Figure 11a to Figure 11c are in accordance with the calculated values from the equations (31) and (32). According to Figure 11, it is clear that from winding turns 1:2:3 to 5:1:3 the magnetizing currents increased which is in consistent with the calculations from (26). It can be pointed out that although much lower current ripples can be achieved with the ratio of 5:1:3, but in experiment, maybe it is not available and cost effective. It is clear that for the same magnetizing inductance, much wire and probably a larger core should be realized for the 5:1:3 ratio. Hence, a balance should be established between some mentioned parameters for the improved Y-source based dc-dc converter in the design procedure.

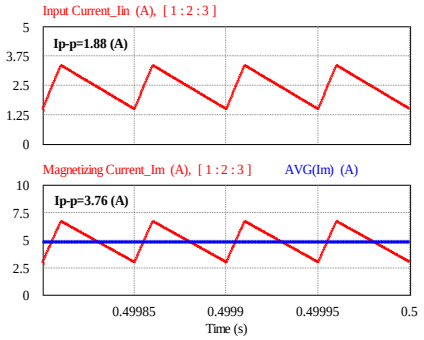

(a)

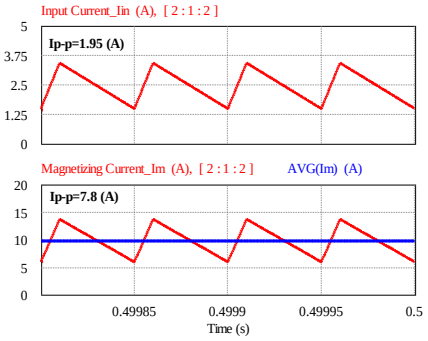

(b)

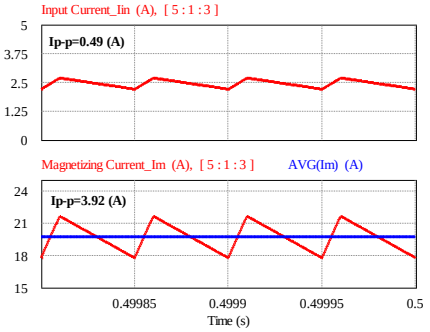

(c)

Figure 11. Input and magnetizing currents for different combination of windings turns and K=4.

5. Experimental Results

A scaled down laboratory prototype of the improved Y-source boost dc-dc converter has been built to validate both theoretical expressions and simulation results. In order to reduce size and weight of the converter, three coupled inductors have been integrated on the same toroid core. The magnetic core used for the prototype is a molypermalloy powder (MPP) core with permeability of 125μ from Dongbu Corporation. Component values and their part numbers that were used for the experiment are listed in Table 3. It should pointed out that a current probe was not available for digital scope at the time of experiment, thus in order to better show input current with lower parasitic effects, switching frequency has been set to 20 kHz. Experimental results recorded from a 150 MHz Yokogawa (DL1540) digital scope. A photo of the laboratory prototype is depicted in Figure 12.

Table 3. Experimental Values and Part numbers

Parameters/Description	Value/Part Number
Power rating	100 W
Input voltage	40 V
Output voltage	200 V
Capacitor C_1	100 μF
Capacitor C_2 and C_3	330 μF
Turns Ratio of Coupled Inductors ($N_1 : N_2 : N_3$)	2:1:2 = 46:23:46 on M200152A core
Winding Factor (K)	4
Duty Cycle (d_{ST})	0.2
Switching Frequency (f_s)	20 kHz
Switch SW	IRFP460A
Diode D1	BYV08
Diode D2	MUR860

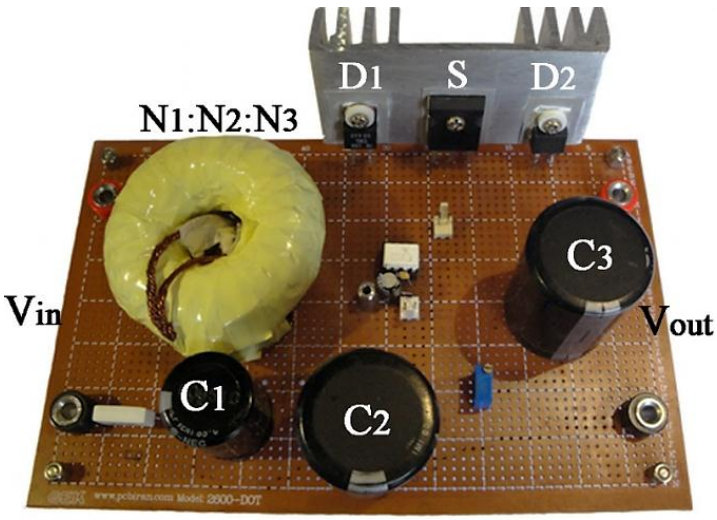

Figure 12. Experimental setup of the improved Y-source boost dc-dc converter.

Figure 13 illustrates experimental results obtained from the Y-source and quasi-Y-source boost dc-dc converters. In which the drain source voltage of switches are shown in top and the input currents are shown in bottom. It can be seen that the input current in both converters are

pulsating and experimental results that observed in laboratory are in good accordance with the simulation results.

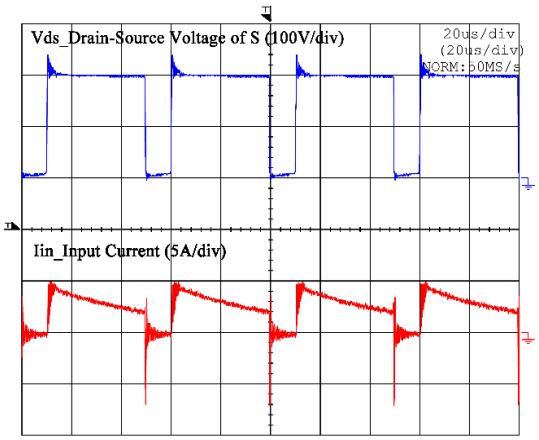

(a)

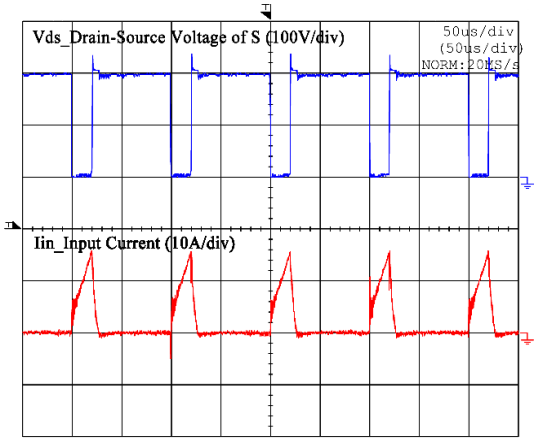

(b)

Figure 13. Experimental results for (a) Y-source based dc-dc converter and (b) quasi-Y-source based dc-dc converter.

Experimental results observed from the improved Y-source boost dc-dc converter using components listed in Table 3 are depicted in Figure 14. As well as the simulation results, the proposed converter draws a continuous input current. Measured magnetizing inductance from the second winding was about 120μH. from (21) and other parameters mentioned in Table 2, the input current ripple can be calculated as 3.33 A. Obviously, the input current ripple can be lowered by employing more winding turns on a larger core. Furthermore, it is evident that the voltage stress across capacitors C_1 and C_2 that observe in Figure 14 are in consistent with previous calculations. Moreover, the ability to achieve a continuous input current in the proposed improved Y-source based converter is verified by the experimental results.

The efficiency of the proposed converter with different load levels is depicted in Figure 15. Notably, the relatively low efficiency of the laboratory prototype is mainly related to its loosely connections (low graded wires and busbars) and internal parasitic elements of the circuit components (Equivalent Series Resistance (ESR) of capacitors and losses related to the semiconductors). However, the proposed converter can achieve more than 90% conversion

efficiency under load variations. Indeed the experimental evaluation focuses on validation of theoretical expressions and simulation results not achieving high-end efficiency.

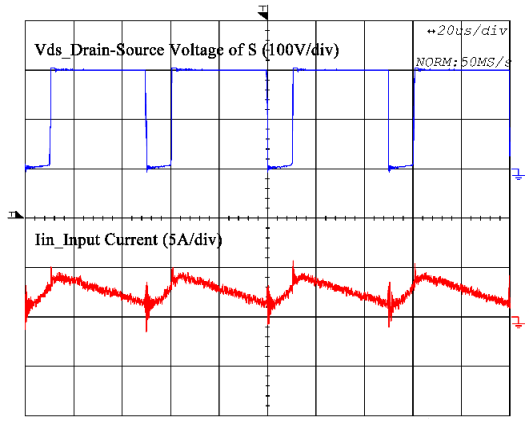

(a)

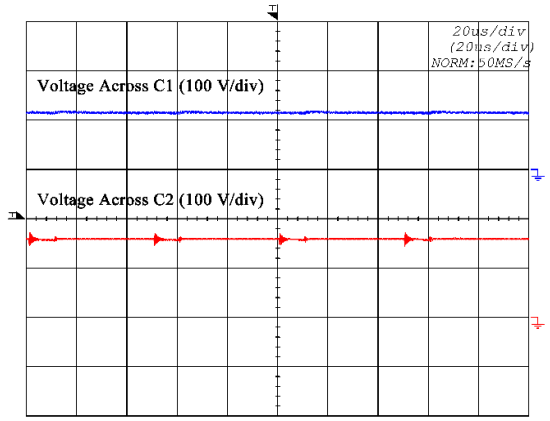

(b)

Figure 14. Experimental results for improved Y-source boost dc-dc converter, (a) the drain-source voltage of switch SW and the input current (b) the voltage across Capacitors.

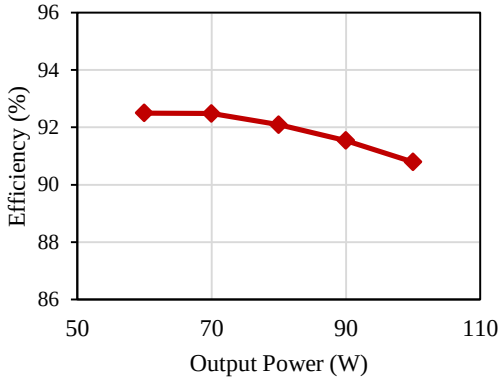

Figure 15. Measured efficiency of the proposed converter.

6. Conclusions

A new Y-source boost dc-dc converter with high voltage gain and a continuous input current introduced in this paper. The proposed converter is intended for applications with varying and low input voltage sources as photovoltaic and fuel cells. Moreover, the proposed converter uses a novel improved Y-source impedance network in its circuit. Steady state analysis and operation principles of developed impedance networks documented in the paper. Furthermore, it is found that the input current ripple of the improved Y-source can vary by different combinations of winding turns. Computer simulations using PSIM software verified the performance of the proposed converter and validated the mathematical derivations. Experimental results from a 100W laboratory prototype also demonstrated the proof of all mentioned characteristics for the proposed converter.

7. References

[1]. F. Blaabjerg, Z. Chen, and S. B. Kjaer, "Power electronics as efficient interface in dispersed power generation systems," *IEEE Trans. Power Electron.*, vol. 19, no. 5, pp. 1184-1194, Sept. 2004.

[2]. J. Dawidziuk, "Review and comparison of high efficiency high power boost DC/DC converters for photovoltaic applications," *Bulletin of the Polish Academy of Sciences: Tech. Sci.*, vol. 59, no. 4, pp. 499-506, Feb. 2012.

[3]. W. Li, X. Lv, Y. Deng, J. Liu, and X. He, "A review of non-isolated high step-up DC/DC converters in renewable energy applications," *24th Annu. Appl. Power Electron. Conf. and Expo. (APEC)*, Washington, DC, 2009, pp. 364-369.

[4]. Q. Zhao and F. C. Lee, "High-efficiency, high step-up DC-DC converters," *IEEE Trans. Power Electron.*, vol. 18, no. 1, pp. 65-73, Jan. 2003.

[5]. B.-R. Lin and J.-J. Chen, "Analysis and implementation of a soft switching converter with high-voltage conversion ratio," *IET Power Electron.*, vol. 1, no. 3, pp. 386-394, Sept. 2008.

[6]. J.-W. Baek, M.-H. Ryoo, T.-J. Kim, D.-W. Yoo, and J.-S. Kim, "High boost converter using voltage multiplier," *31st Annu. Conf. Ind. Electron. Soc. (IECON)*, 2005, p. 6 pp.

[7]. W. Yu, C. Hutchens, J.-S. Lai, J. Zhang, G. Lisi, A. Djabbari, *et al.*, "High efficiency converter with charge pump and coupled inductor for wide input photovoltaic AC module applications," *Energy Conv. Congr. and Expo. (ECCE)*, San Jose, CA, 2009, pp. 3895-3900.

[8]. K. Yari, M. Forouzesh, and A. Baghramian, "A novel high voltage gain DC-DC converter with reduced components voltage stress," *6th Power Electron., Drives Sys. & Tech. Conf. (PEDSTC)*, Tehran, 2015, pp. 173-177.

[9]. F. Z. Peng, "Z-source inverter," *IEEE Trans. Ind. Appl.*, vol. 39, no. 2, pp. 504-510, Mar/Apr 2003.

[10]. T. Takiguchi and H. Koizumi, "Quasi-Z-source dc-dc converter with voltage-lift technique," *39th Annu. Conf. Ind. Electron. Soc. (IECON)*, Vienna, 2013, pp. 1191-1196.

[11]. D. Vinnikov, I. Roasto, R. Strzelecki, and M. Adamowicz, "Step-up DC/DC converters with cascaded quasi-Z-source network," *IEEE Trans. Ind. Electron.*, vol. 59, no. 10, pp. 3727-3736, Oct. 2012.

[12]. D. Vinnikov, I. Roasto, R. Strzelecki, and M. Adamowicz, "Performance improvement method for the voltage-fed qZSI with continuous input current," *15th Mediterranean Electrotechnical Conf. (MELECON)*, Valletta, 2010, pp. 1459-1464.

[13]. D. Cao and F. Z. Peng, "A family of Z-source and quasi-Z-source DC-DC converters," *24th Annu. Appl. Power Electron. Conf. and Expo. (APEC)*, Washington, DC, 2009, pp. 1097-1101.

[14]. W. Qian, F. Z. Peng, and H. Cha, "Trans-Z-source inverters," *IEEE Trans. Power Electron.*, vol. 26, no. 12, pp. 3453-3463, Dec. 2011.

[15]. P. C. Loh, D. Li, and F. Blaabjerg, "Γ-Z-source inverters," *IEEE Trans. Power Electron.*, vol. 28, no. 11, pp. 4880-4884, Nov. 2013.

[16]. Y. P. Siwakoti, P. C. Loh, F. Blaabjerg and G. E. Town, "Y-Source Impedance Network," *IEEE Trans. Power Electron.*, vol. 29, no. 7, pp. 3250-3254, July 2014.
[17]. S. K. Mazumder, R. K. Burra, and K. Acharya, "A ripple-mitigating and energy-efficient fuel cell power-conditioning system," *IEEE Trans. Power Electron.*, vol. 22, no. 4, pp. 1437-1452, July 2007.
[18]. A. E. Khateb, N. A. Rahim, J. Selvaraj, and B. W. Williams, "The effect of input current ripple on the photovoltaic panel efficiency," *Clean Energy and Tech. (CEAT)*, Lankgkawi, 2013, pp. 478-481.
[19]. M. K. Nguyen, Y. C. Lim, and S.-J. Park, "Improved trans-Z-source inverter with continuous input current and boost inversion capability," *IEEE Trans. Power Electron*, vol. 28, no. 10, pp. 4500-4510, Oct. 2013.
[20]. W. Mo, P. C. Loh, and F. Blaabjerg, "Voltage Type Γ-source Inverters with Continuous Input Current and Enhanced Voltage Boost Capability," *15th Int. Power Electron. and Motion Cont. Conf. (EPE/PEMC)*, Novi Sad, 2012, pp. LS5d.2-1-LS5d.2-8.
[21]. M. Forouzesh and A. Baghramian, "High voltage gain Y-source based isolated DC-DC converter with continuous input current," *6th Power Electron., Drives Sys. & Tech. Conf. (PEDSTC)*, Tehran, 2015, pp. 453-457.
[22]. Y. P. Siwakoti, P. C. Loh, F. Blaabjerg and G. E. Town, "Effects of Leakage Inductances on Magnetically Coupled Y-Source Network," *IEEE Trans. Power Electron.*, vol. 29, no. 11, pp. 5662-5666, Nov. 2014.

Mojtaba Forouzesh received the B.S. degree in Physics from the University of Guilan, Rasht, Iran, in 2011, and the M.S. degree in electrical engineering with first class honors from the same institute in 2015.
He is currently a graduate researcher at the Department of Electrical Engineering, the University of Guilan. His major research interests include magnetically coupled impedance source based converters/inverters, high step-up dc-dc converters, renewable energy technologies and applications, small signal modeling of power converters and digital implementation of modulation and control schemes.

Alfred Baghramian was born in Iran 1969, received the B.Sc. degree in electrical engineering from Isfahan University of Technology, Isfahan, Iran, in 1991; M.Sc. degree in electrical engineering from The University of Tarbiat-Modarres, Tehran- Iran, in 1994 and the Ph.D. degree in power electronics from the University of Birmingham, Birmingham, U.K., in 2006.
His research interests include high-frequency power converters, high power-factor rectification and the modeling and control of autonomous power systems. Dr. Alfred Baghramian has been a Lecturer at The University of Guilan, Rasht-Iran Since 1994.